Instituto de Física de Cantabria

UNIVERSITY OF CAMBRIDGE
Astrophysics Group
Cavendish Laboratory

Kavli Institute for Cosmology Cambridge
KICC

Forecasts on the contamination induced by unresolved point sources in primordial NG beyond Planck

Andrés Curto et al.

MNRAS 2013, 432, 728 (arXiv:1301.1544)

Overview

- Extra-galactic point sources
  - Radio sources
  - Infra-red sources
    - Late type
    - Spheroids
    - Lensed spheroids
- Point source power spectrum
  - Number counts and power spectra for different populations
  - Impact of the flux cut S_c
  - Comparison with the CMB power spectrum
- Point source bispectrum
  - Bispectrum for different populations of sources (temperature and polarization)
- f_{nl} estimates
  - The bias due to the point sources $\Delta(f_{nl})$
  - The uncertainties including point sources $\sigma(f_{nl})$

CMB formalism

CMB anisotropies

$$X_i(\vec{n}) = \sum_{\ell m} a^i_{\ell m} Y_{\ell m}(\vec{n}) \qquad X_i = \{T, E, B\}$$

Power spectrum

$$C_\ell \delta_{\ell\ell'} \delta_{mm'} = \left\langle a_{\ell m} a^*_{\ell' m'} \right\rangle$$

Bispectrum

$$B^{m_1 m_2 m_3}_{\ell_1 \ell_2 \ell_3} = \left\langle a_{\ell_1 m_1} a_{\ell_2 m_2} a_{\ell_3 m_3} \right\rangle$$

Angle averaged bispectrum

$$B_{\ell_1 \ell_2 \ell_3} = \sum_{m_1 m_2 m_3} B^{m_1 m_2 m_3}_{\ell_1 \ell_2 \ell_3} \begin{pmatrix} m_1 & m_2 & m_3 \\ \ell_1 & \ell_2 & \ell_3 \end{pmatrix}$$

Reduced bispectrum

$$B_{\ell_1 \ell_2 \ell_3} = b_{\ell_1 \ell_2 \ell_3} \sqrt{\frac{(2\ell_1+1)(2\ell_2+1)(2\ell_3+1)}{4\pi}} \begin{pmatrix} \ell_1 & \ell_2 & \ell_3 \\ 0 & 0 & 0 \end{pmatrix}$$

Extragalactic Point Sources

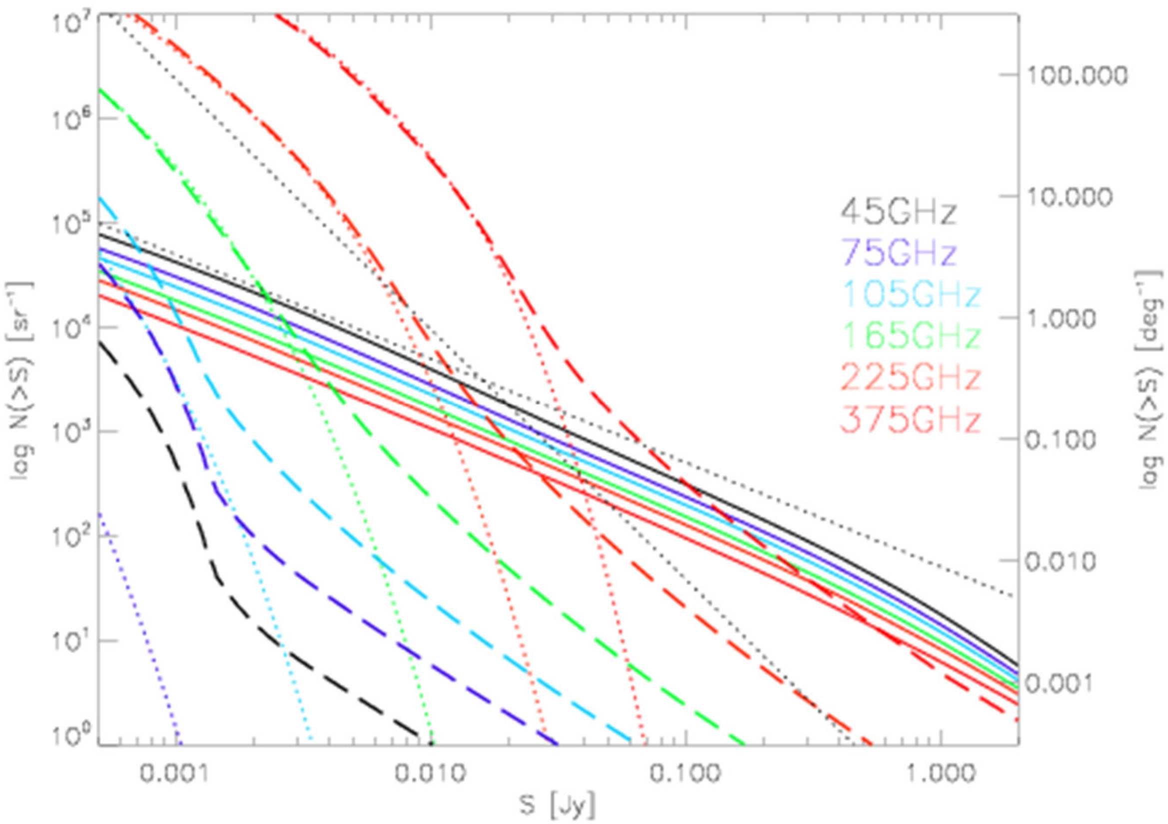

Predicted number counts

- Radio sources: solid lines, model by Tucci et al (2011)
- Far-Infrared sources: dashed lines for total counts and dotted lines for proto-spheroidal galaxies, model by Lapi et al (2011)

Power Spectra from Poisson distributed Point Sources

- **Temperature PS**

$$C_{T\ell} = \left(\frac{dB}{dT}\right)^2 N\langle S^2\rangle = \left(\frac{dB}{dT}\right)^2 \int_0^{S_c} n(S)S^2 dS$$

- **Polarization PS**

$$C_{Q\ell} \approx C_{U\ell} \approx C_{E\ell} \approx C_{B\ell}$$

$$C_{Q\ell} = \left(\frac{dB}{dT}\right)^2 N\langle Q^2\rangle = \left(\frac{dB}{dT}\right)^2 N\langle S^2 \Pi^2 \cos^2(2\varphi)\rangle = \frac{1}{2}\langle \Pi^2\rangle C_{T\ell}$$

- **Cross PS (Temperature-Polarization)**

$$C_{TQ\ell} = \left(\frac{dB}{dT}\right)^2 \langle S^2 \Pi \cos(2\varphi)\rangle = 0$$

Radio sources are Poissonian distributed
IR sources are spatially correlated
We use Argüeso et al (2003) prescription

Polarization of Point Sources

The typical linear polarization degree (Π) is a **few per cent**, indication of a low order of magnetic fields.

Polarization parameters for radio sources (Tucci & Toffolatti 2012):

	Π_{med}	$<\Pi^2>^{1/2}$
Steep	4%	6%
FSRQ	3%	3.8%
BLLac	3.6%	4.5%

Polarization parameters for far-IR sources (few data so far collected):

average polarization level of 1 %

Point source power spectrum

B-mode with
r = 0.1, 0.01, 10^{-3}

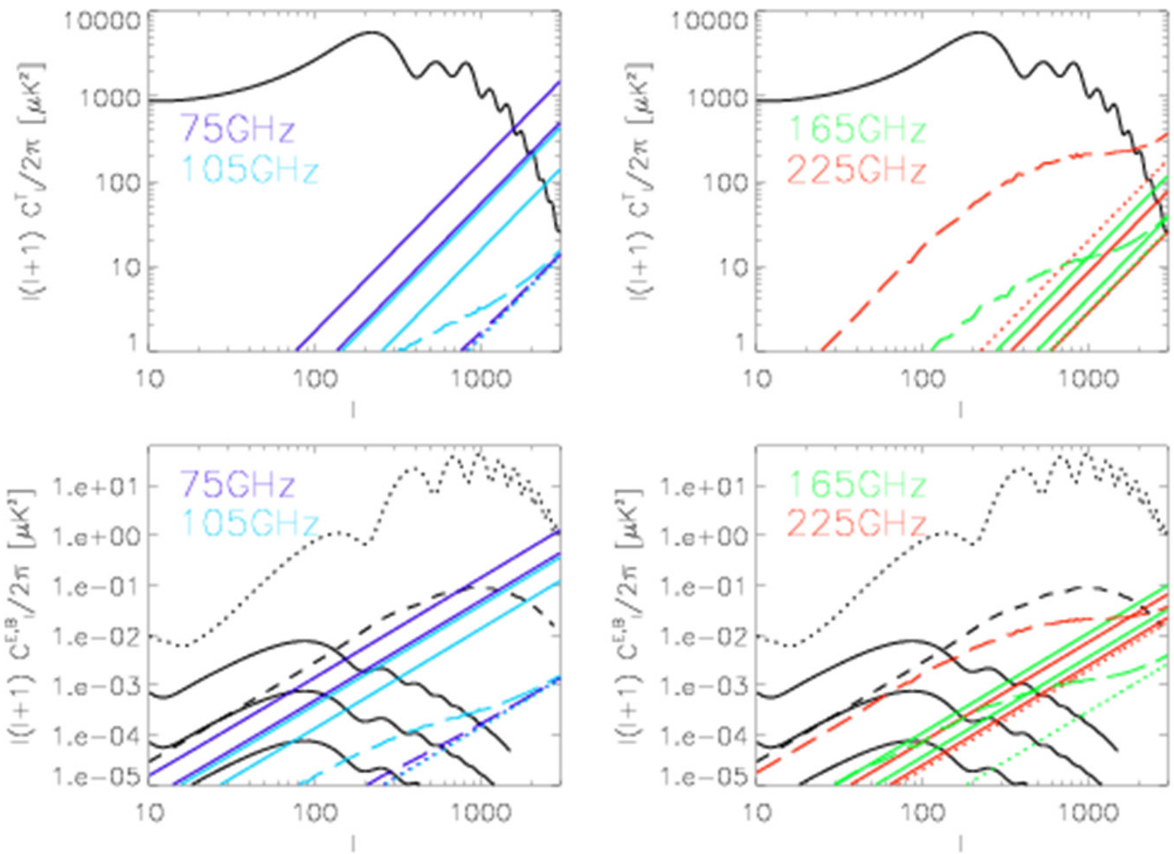

Two flux limits
S_{lim} = 0.3 Jy
S_{lim} = 1 Jy

Power spectra

- Radio sources: solid lines, model by Tucci et al (2011)
- Far-Infrared sources: dashed lines for total counts and dotted lines for Poisson contribution, model by Lapi et al (2011)

The PS bispectrum

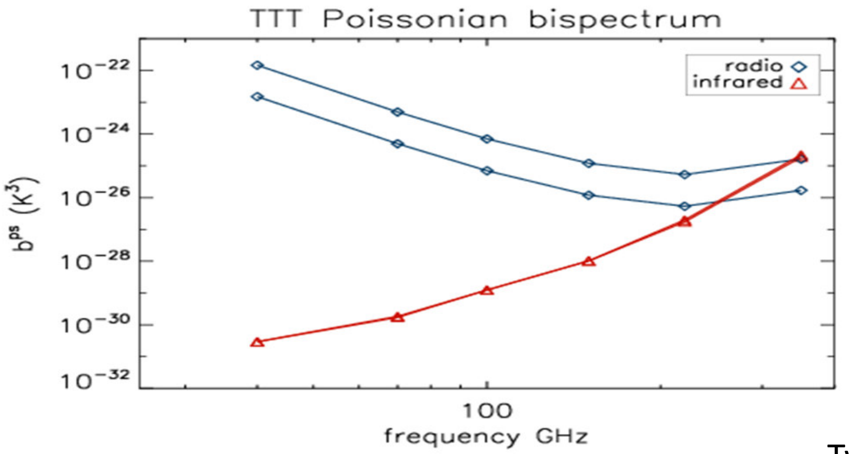

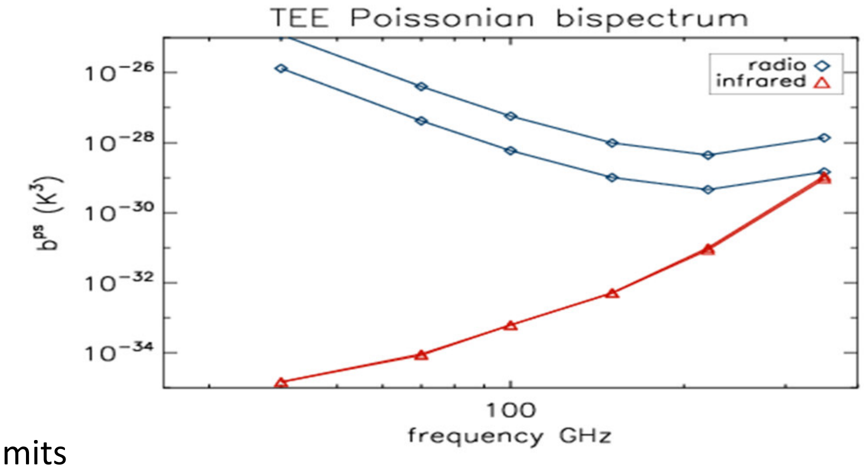

Two flux limits
S_{lim} = 0.3 Jy
S_{lim} = 1 Jy

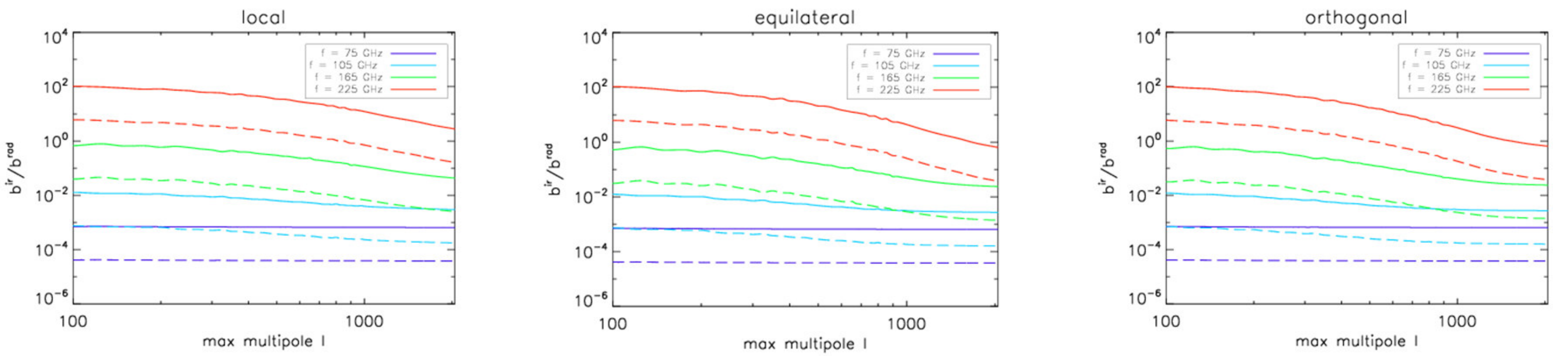

$$B^{PS}_{\ell_1\ell_2\ell_3} = B^{radio} + B^{ir,poiss}\sqrt{\frac{C^{ir}_{\ell_1}C^{ir}_{\ell_2}C^{ir}_{\ell_3}}{C^{ir,poiss}_{\ell_1}C^{ir,poiss}_{\ell_2}C^{ir,poiss}_{\ell_3}}}$$

The bispectrum including polarization can be defined in an equivalent way (considered components **TTT, TEE, TBB**). The remaining components are equal to zero.

Primordial non-Gaussianity

- Considered f_{nl} shapes
  - Local
  - Equilateral
  - Orthogonal
  - Flat

Local shape

- Shape function:

$$F(k_1,k_2,k_3)=2\Delta_\Phi^2 f_{nl}\left[\frac{1}{k_1^{3-(n_s-1)}k_2^{3-(n_s-1)}}+\frac{1}{k_1^{3-(n_s-1)}k_3^{3-(n_s-1)}}+\frac{1}{k_2^{3-(n_s-1)}k_3^{3-(n_s-1)}}\right]$$

- This signal peaks in squeezed configurations: $k_1 \approx k_2 >> k_3$

$$F(1,x_2,x_3)x_2^2x_3^2 / F(1,1,1)$$

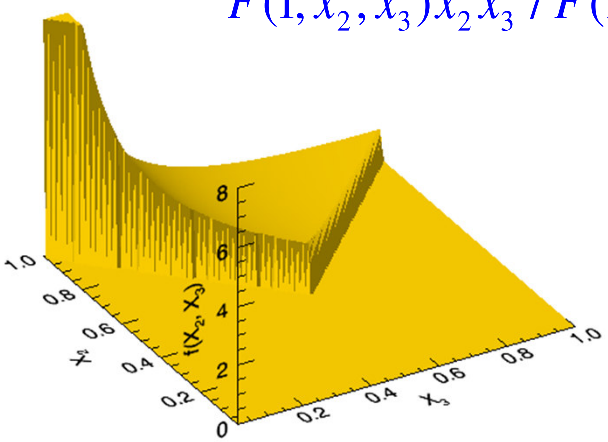

$x_3 = k_3 / k_1$ $\qquad$ $x_2 = k_2 / k_1$

Equilateral shape

- Shape function:

$$F(k_1,k_2,k_3)=6\Delta_\Phi^2 f_{nl}\left[-\frac{1}{k_1^{3-(n_s-1)}k_2^{3-(n_s-1)}}+(2\,perm.)-\frac{2}{(k_1k_2k_3)^{2-2(n_s-1)/3}}+\frac{1}{k_1^{1-(n_s-1)}k_2^{2-(n_s-1)}k_3^{3-(n_s-1)}}+(5\,perm.)\right]$$

- This signal peaks in *equilateral* configurations: $k_1 \approx k_2 \approx k_3$

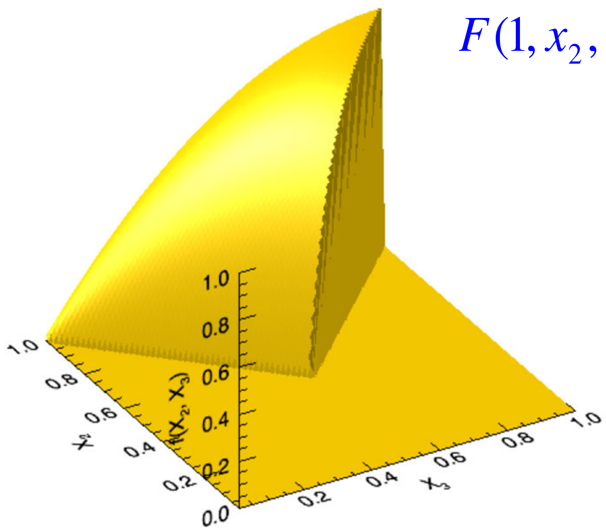

$$F(1,x_2,x_3)x_2^2x_3^2\,/\,F(1,1,1)$$

$x_3 = k_3 / k_1$ $\qquad$ $x_2 = k_2 / k_1$

Orthogonal shape

- Shape function:

$$F(k_1,k_2,k_3)=6Af_{nl}$$

$$\times\left\{-\frac{3}{k_1^{4-n_s}k_2^{4-n_s}}-\frac{3}{k_2^{4-n_s}k_3^{4-n_s}}-\frac{3}{k_3^{4-n_s}k_1^{4-n_s}}-\frac{8}{(k_1k_2k_3)^{2(4-n_s)/3}}+\left[\frac{3}{k_1^{4-n_s}k_2^{4-n_s}k_3^{4-n_s}}+(5\ perm.)\right]\right\}$$

- This signal peaks in *equilateral* $k_1 \approx k_2 \approx k_3$ and flat $k_1 = k_2 + k_3$

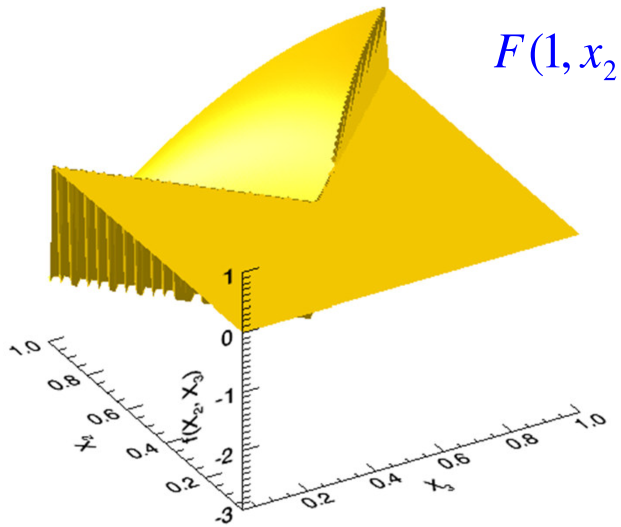

$$F(1,x_2,x_3)x_2^2x_3^2\,/\,F(1,1,1)$$

$x_3 = k_3 / k_1$ $\qquad$ $x_2 = k_2 / k_1$

Flat shape

- Shape function:

$$F(k_1,k_2,k_3)=6Af_{nl}$$

$$\times\left\{-\frac{3}{k_1^{4-n_s}k_2^{4-n_s}}-\frac{3}{k_2^{4-n_s}k_3^{4-n_s}}-\frac{3}{k_3^{4-n_s}k_1^{4-n_s}}-\frac{8}{(k_1k_2k_3)^{2(4-n_s)/3}}+\left[\frac{3}{k_1^{4-n_s}k_2^{4-n_s}k_3^{4-n_s}}+(5\ perm.)\right]\right\}$$

- This signal peaks in flat $k_1 = k_2 + k_3$ configurations

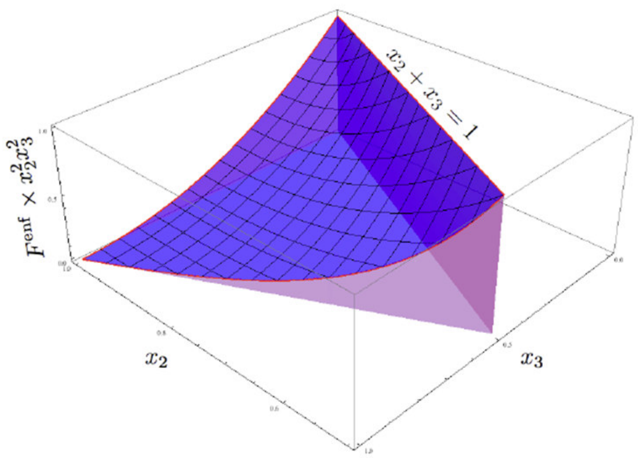

Figure 4. The enfolded template shape $F(x_2, x_3) \times x_2^2 x_3^2$.

$$F(1,x_2,x_3)x_2^2x_3^2\,/\,F(1,1,1)$$

Image from arXiv:0901.4044

$$x_3 = k_3/k_1 \qquad x_2 = k_2/k_1$$

Primordial non-Gaussianity f_{nl} bias estimator (T)

$$\Delta f_{nl} = \frac{\displaystyle\sum_{\ell_1 \le \ell_2 \le \ell_3 \le \ell_{\max}} \frac{B^{ps}_{\ell_1 \ell_2 \ell_3} B^{prim}_{\ell_1 \ell_2 \ell_3}}{\Delta_{\ell_1 \ell_2 \ell_3} C_{\ell_1} C_{\ell_2} C_{\ell_3}}}{\displaystyle\sum_{\ell_1 \le \ell_2 \le \ell_3 \le \ell_{\max}} \frac{B^{prim}_{\ell_1 \ell_2 \ell_3} B^{prim}_{\ell_1 \ell_2 \ell_3}}{\Delta_{\ell_1 \ell_2 \ell_3} C_{\ell_1} C_{\ell_2} C_{\ell_3}}} \qquad \sigma^2(f_{nl}) = \frac{1}{\displaystyle\sum_{\ell_1 \le \ell_2 \le \ell_3 \le \ell_{\max}} \frac{B^{prim}_{\ell_1 \ell_2 \ell_3} B^{prim}_{\ell_1 \ell_2 \ell_3}}{\Delta_{\ell_1 \ell_2 \ell_3} C_{\ell_1} C_{\ell_2} C_{\ell_3}}}$$

Total power spectrum

$$C_\ell = \left(C_\ell^{CMB} + C_\ell^{IR\,PS} + C_\ell^{Radio\,PS}\right) b_\ell^2 w_\ell^2 + C_\ell^{noise}$$

CMB power spectrum

Infra-red point source power spectrum

radio point source power spectrum

Instrumental noise

Primordial non-Gaussianity f_{nl} bias estimator (T and E)

$$\Delta f_{nl} = \frac{\sum_{ijk,rst,\ell_1\le\ell_2\le\ell_3\le\ell_{\max}} B^{ijk,ps}_{\ell_1\ell_2\ell_3} C^{-1}_{ijk,rst} B^{rst,prim}_{\ell_1\ell_2\ell_3}}{\sum_{ijk,rst,\ell_1\le\ell_2\le\ell_3\le\ell_{\max}} B^{ijk,prim}_{\ell_1\ell_2\ell_3} C^{-1}_{ijk,rst} B^{rst,prim}_{\ell_1\ell_2\ell_3}} \qquad \sigma^2(f_{nl}) = \frac{1}{\sum_{ijk,rst,\ell_1\le\ell_2\le\ell_3\le\ell_{\max}} B^{prim}_{\ell_1\ell_2\ell_3} C^{-1}_{ijk,rst} B^{prim}_{\ell_1\ell_2\ell_3}}$$

Indices i, j, k, r, s, t = {T, E}

Power spectrum covariance

$$C_{ijk,pqr} = C^{ip}_{\ell_1} C^{jq}_{\ell_2} C^{kr}_{\ell_3} + C^{ip}_{\ell_1} C^{jr}_{\ell_2} C^{kq}_{\ell_3} \delta_{\ell_2\ell_3} + C^{ir}_{\ell_1} C^{jq}_{\ell_2} C^{kp}_{\ell_3} \delta_{\ell_1\ell_3} + C^{iq}_{\ell_1} C^{jp}_{\ell_2} C^{kr}_{\ell_3} \delta_{\ell_1\ell_2} + \\ + C^{iq}_{\ell_1} C^{jr}_{\ell_2} C^{kp}_{\ell_3} \delta_{\ell_1\ell_2} \delta_{\ell_2\ell_3} \delta_{\ell_1\ell_3} + C^{ir}_{\ell_1} C^{jp}_{\ell_2} C^{kq}_{\ell_3} \delta_{\ell_1\ell_3} \delta_{\ell_2\ell_1} \delta_{\ell_2\ell_3}$$

Polarization non-zero point source power spectrum and bispectrum (even number of E)

$$b^{TEE} = \langle p^2 \rangle \langle \cos^2(2\phi) \rangle b^{TTT} \qquad b^{TTE} = b^{EEE} = 0$$

Characteristic parameters for a future CMB mission

Freq (GHz)	45	75	105	165	225	375
Beam FWHM	23.3	14.0	10.0	6.4	4.7	2.8
Temp: σ_{noise} (μK·arcmin)	5.25	2.73	2.68	2.67	2.64	68.6
Pol: σ_{noise} (μK·arcmin)	9.07	4.72	4.63	4.61	4.57	119

Parameters from COrE white paper http://arxiv.org/abs/1102.2181

- Considered two flux limits for each frequency:

  S_{lim} = 0.3 Jy
  S_{lim} = 1 Jy

- Maximum multipole l_{max} = 2048
- Considered cases:
  - Ideal conditions
  - COrE (2011) instrumental conditions

Expected uncertainties in f_{nl}

(Ideal conditions)

AC, M. Tucci et al. (2013)

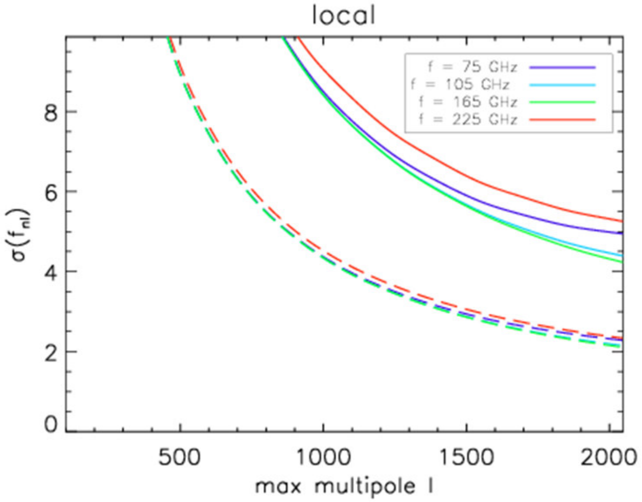

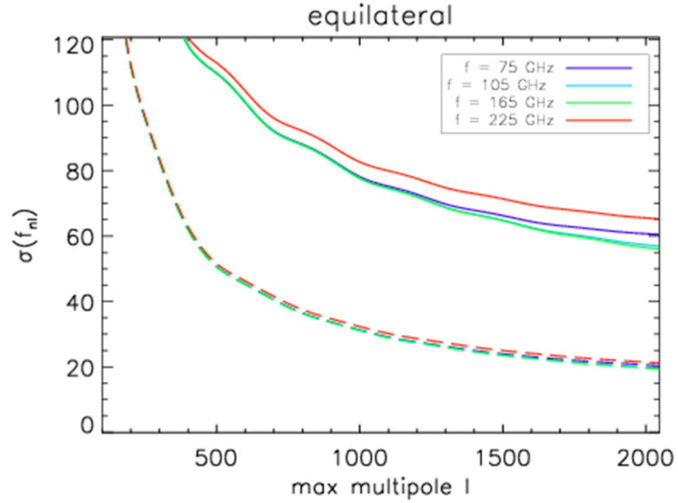

S_{lim} = 0.3 Jy

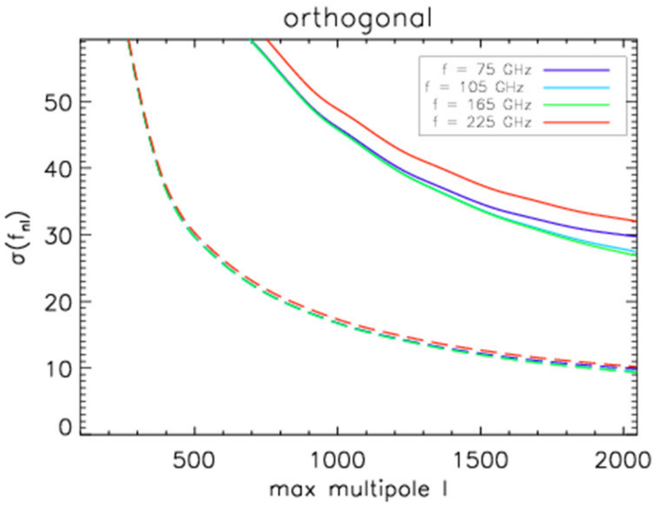

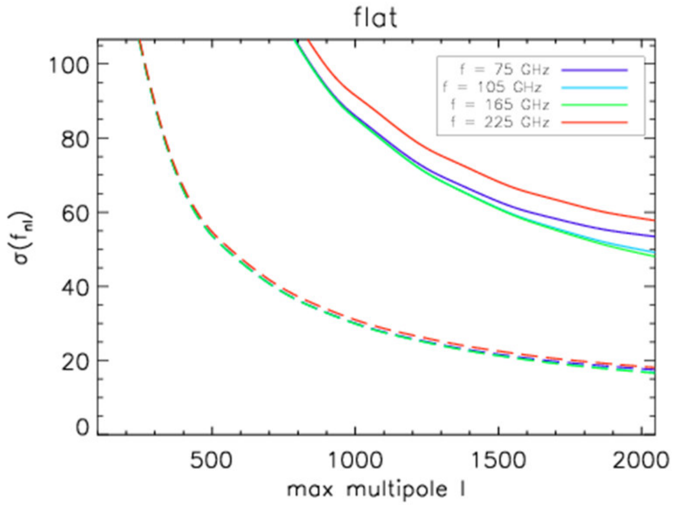

Solid lines: T
Dashed lines: T and E

Point source contamination to f_{nl}

(Ideal conditions)

AC, M. Tucci et al. (2013)

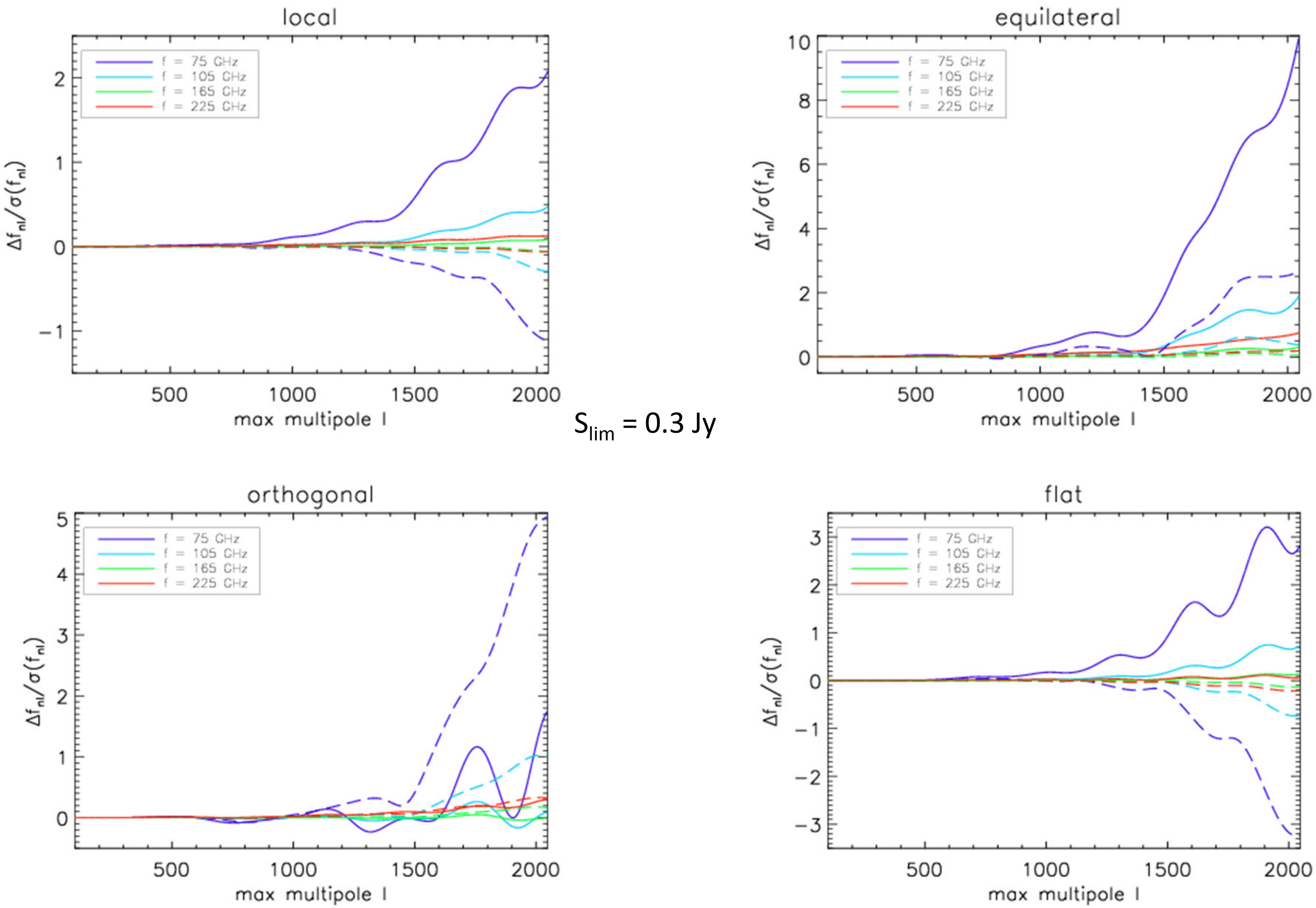

S_{lim} = 0.3 Jy

Solid lines: T

Dashed lines: T and E

Expected uncertainties in f_{nl}

(COrE conditions)

AC, M. Tucci et al. (2013)

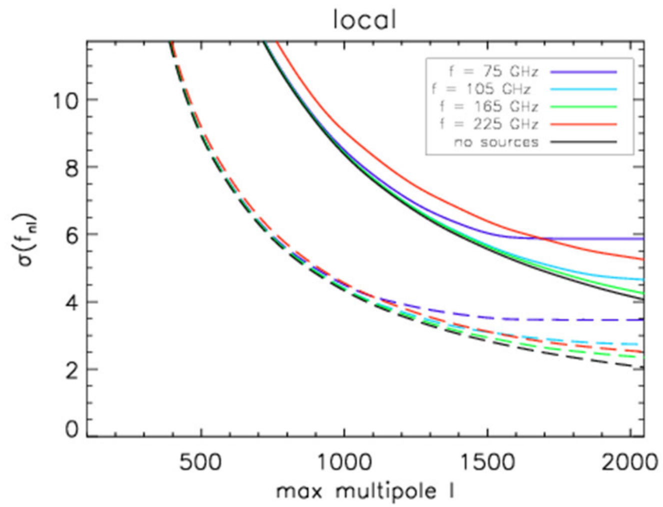

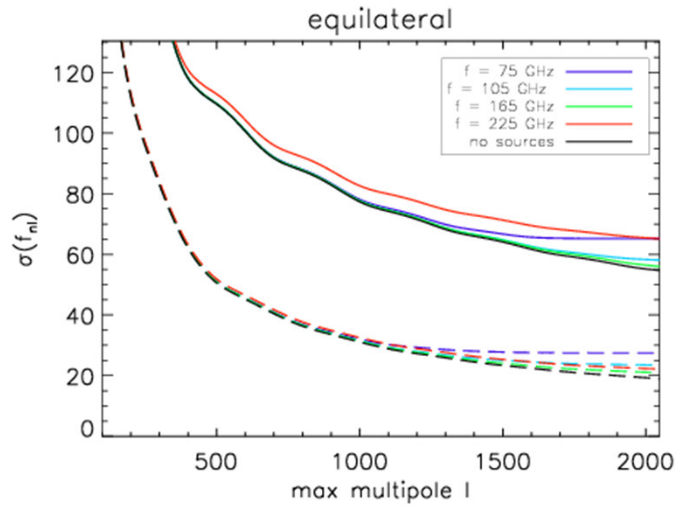

S_{lim} = 0.3 Jy

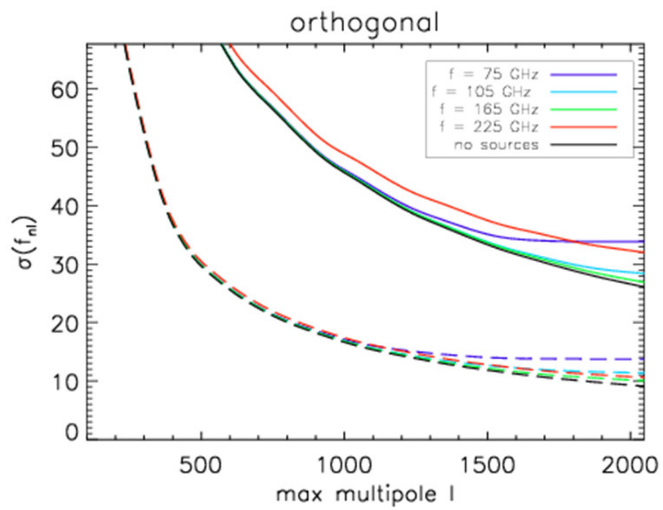

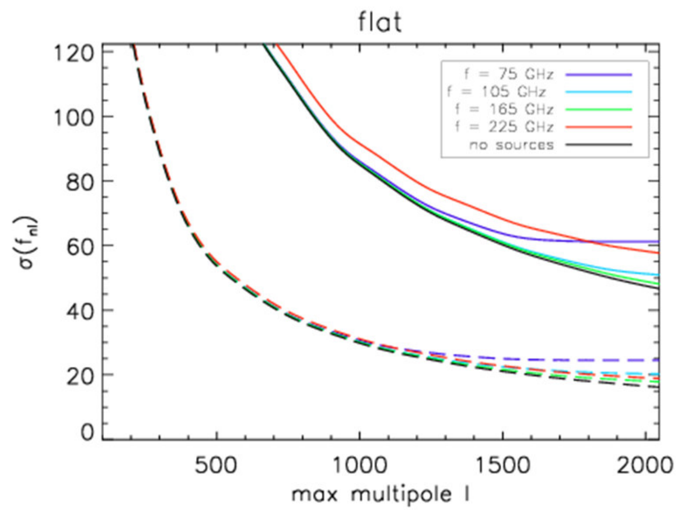

Solid lines: T
Dashed lines: T and E

Point source contamination to f_{nl}

(COrE conditions)

AC, M. Tucci et al. (2013)

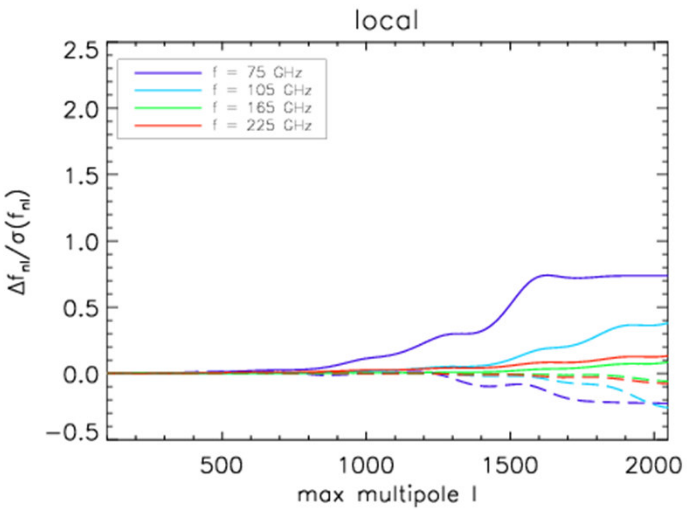

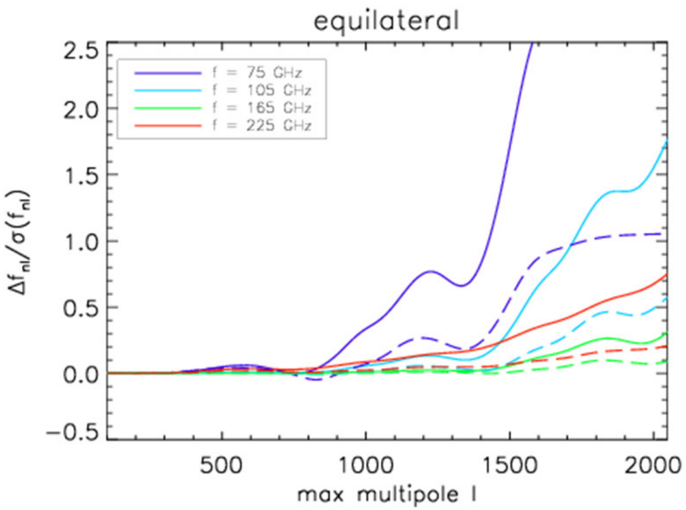

S_{lim} = 0.3 Jy

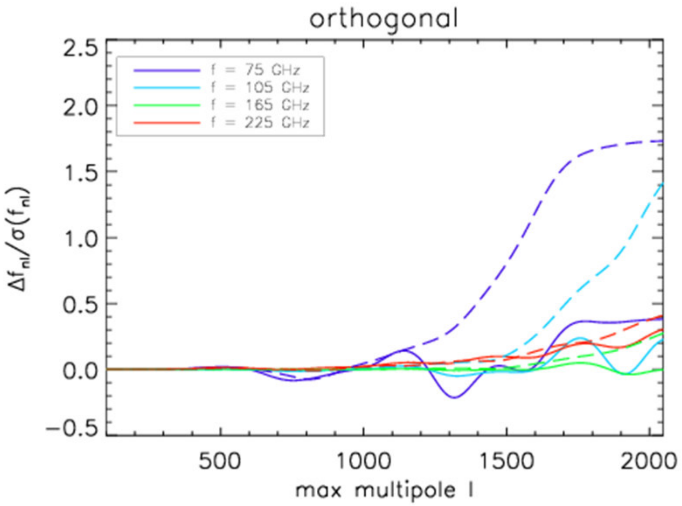

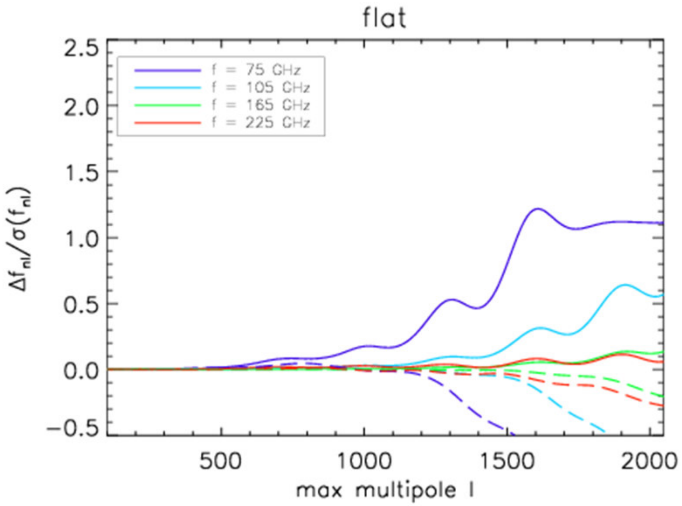

Solid lines: T
Dashed lines: T and E

Expected uncertainties in f_{nl}

(Ideal conditions)

AC, M. Tucci et al. (2013)

Table 2. The expected uncertainty $\sigma(f_{nl})$, bias Δf_{nl} and relative bias $\Delta f_{nl}/\sigma(f_{nl})$ at $\ell_{max} = 2048$ from temperature only and temperature plus polarization for an ideal mission. S_c =0.3Jy is taken.

	case Freq.	T 45	T 75	T 105	T 165	T 225	T 375	T+E 45	T+E 75	T+E 105	T+E 165	T+E 225	T+E 375
local	$\sigma(f_{nl})$	7.4	4.9	4.4	4.2	5.2	29.7	2.8	2.3	2.1	2.1	2.3	3.3
	Δf_{nl}	82.1	10.3	2.1	0.4	0.7	25.6	-9.7	-2.6	-0.6	-0.1	-0.1	-0.1
	$\Delta f_{nl}/\sigma(f_{nl})$	11.1	2.1	0.5	0.1	0.1	0.9	-3.5	-1.1	-0.3	-0.1	-0.1	-0.0
equilateral	$\sigma(f_{nl})$	75.4	60.4	56.8	55.9	65.1	232.4	24.0	20.3	19.5	19.2	21.1	35.3
	Δf_{nl}	4629.3	599.9	107.2	17.2	49.1	950.7	480.2	54.5	7.3	0.8	4.0	17.9
	$\Delta f_{nl}/\sigma(f_{nl})$	61.4	9.9	1.9	0.3	0.8	4.1	20.0	2.7	0.4	0.0	0.2	0.5
orthogonal	$\sigma(f_{nl})$	40.1	29.7	27.4	26.8	32.0	139.0	11.6	9.8	9.4	9.2	10.1	16.5
	Δf_{nl}	955.5	51.7	2.5	-0.2	9.7	371.4	308.7	48.3	9.4	1.6	3.4	7.2
	$\Delta f_{nl}/\sigma(f_{nl})$	23.8	1.7	0.1	-0.0	0.3	2.7	26.7	4.9	1.0	0.2	0.3	0.4
flat	$\sigma(f_{nl})$	73.7	53.3	49.0	47.9	57.6	284.7	20.6	17.4	16.6	16.4	17.9	29.1
	Δf_{nl}	598.6	150.5	36.0	6.7	3.4	-66.0	-311.6	-56.3	-12.2	-2.2	-3.9	-5.2
	$\Delta f_{nl}/\sigma(f_{nl})$	8.1	2.8	0.7	0.1	0.1	-0.2	-15.1	-3.2	-0.7	-0.1	-0.2	-0.2

S_{lim} = 0.3 Jy

AC, M. Tucci et al. (2013) (arXiv:1301.1544)

Expected uncertainties in f_{nl}

(COrE conditions)

AC, M. Tucci et al. (2013)

Table 4. The expected uncertainty $\sigma(f_{\rm nl})$, bias $\Delta f_{\rm nl}$ and relative bias $\Delta f_{\rm nl}/\sigma(f_{\rm nl})$ at $\ell_{\rm max} = 2048$ from temperature only and temperature plus polarization for a *COrE*-like mission. $S_c = 0.3$ Jy is adopted.

	Case Freq.	T 45	T 75	T 105	T 165	T 225	T 375	$T+E$ 45	$T+E$ 75	$T+E$ 105	$T+E$ 165	$T+E$ 225	$T+E$ 375
	$\sigma(f_{\rm nl})$	9.7	5.9	4.7	4.2	5.3	29.8	6.0	3.5	2.7	2.3	2.5	20.6
Local	$\Delta f_{\rm nl}$	16.0	4.3	1.8	0.4	0.7	25.1	1.9	−0.8	−0.7	−0.1	−0.2	8.2
	$\Delta f_{\rm nl}/\sigma(f_{\rm nl})$	1.7	0.7	0.4	0.1	0.1	0.8	0.3	−0.2	−0.3	−0.1	−0.1	0.4
	$\sigma(f_{\rm nl})$	84.3	65.2	58.1	56.0	65.2	232.6	41.1	27.5	23.5	21.0	22.2	147.2
Equilateral	$\Delta f_{\rm nl}$	421.9	202.4	102.7	17.5	49.0	935.9	66.2	28.9	13.5	1.9	4.6	343.8
	$\Delta f_{\rm nl}/\sigma(f_{\rm nl})$	5.0	3.1	1.8	0.3	0.8	4.0	1.6	1.1	0.6	0.1	0.2	2.3
	$\sigma(f_{\rm nl})$	49.7	33.8	28.4	26.9	32.0	139.1	21.7	13.8	11.4	10.1	10.6	82.0
Orthogonal	$\Delta f_{\rm nl}$	39.9	12.9	6.5	−0.1	9.7	367.8	12.1	23.8	16.1	2.8	4.4	130.2
	$\Delta f_{\rm nl}/\sigma(f_{\rm nl})$	0.8	0.4	0.2	−0.0	0.3	2.6	0.6	1.7	1.4	0.3	0.4	1.6
	$\sigma(f_{\rm nl})$	93.8	61.2	50.9	48.1	57.7	285.1	39.1	24.5	20.2	17.9	18.9	148.1
Flat	$\Delta f_{\rm nl}$	190.3	68.1	29.0	6.5	3.4	−68.8	10.4	−26.3	−20.4	−3.7	−5.2	−38.4
	$\Delta f_{\rm nl}/\sigma(f_{\rm nl})$	2.0	1.1	0.6	0.1	0.1	−0.2	0.3	−1.1	−1.0	−0.2	−0.3	−0.3

S_{lim} = 0.3 Jy

AC, M. Tucci et al. (2013) (arXiv:1301.1544)

Conclusions

- Power spectrum of point sources:
  - Temperature: contamination of radio sources is mostly located at multipoles l > 2000
  - Significant contamination for the cosmological B mode at all frequencies if r < 10^{-2}
- Bispectrum of point sources:
  - B_{PS} is zero for odd polarization combinations
  - Radio B_{PS} larger than IR B_{PS} for ν <= 200 GHz (both TTT and TEE)
- Non-Gaussianity: f_{nl} bias:
  - The polarization reduces the bias and the $\sigma(f_{nl})$ on all the considered f_{nl} shapes
  - Negligible bias contamination for 150 < ν < 225 GHz (S_{cut}=0.3 Jy)